AUTOMATED LANDMARKS DETECTION
ON 3D HUMAN FACIAL IMAGE

NGO CHEE GUAN

FACULTY OF SCIENCE
UNIVERSITY OF MALAYA
KUALA LUMPUR

2014

AUTOMATED LANDMARKS DETECTION
ON 3D HUMAN FACIAL IMAGE

NGO CHEE GUAN

SUBMITTED TO THE
INSTITUTE OF BIOLOGICAL SCIENCES
FACULTY OF SCIENCE
UNIVERSITY OF MALAYA, IN PARTIAL FULFILMENT
OF THE REQUIREMENTS FOR THE DEGREE OF
MASTER OF BIOINFORMATICS

2014

<div align="center">

UNIVERSITY OF MALAYA

ORIGINAL LITERARY WORK DECLARATION

</div>

Name of Candidate: NGO CHEE GUAN   (I.C/Passport No: 830723-14-5813)

Registration/Matric No: SGJ130008

Name of Degree: MASTER OF BIOINFORMATICS

Title of Project Paper/Research Report/Dissertation/Thesis ("this Work"):

 AUTOMATED LANDMARKS DETECTION ON 3D HUMAN FACIAL IMAGE

Field of Study: BIOINFORMATICS

 I do solemnly and sincerely declare that:

(1) I am the sole author/writer of this Work;

(2) This Work is original;

(3) Any use of any work in which copyright exists was done by way of fair dealing and for permitted purposes and any excerpt or extract from, or reference to or reproduction of any copyright work has been disclosed expressly and sufficiently and the title of the Work and its authorship have been acknowledged in this Work;

(4) I do not have any actual knowledge nor do I ought reasonably to know that the making of this work constitutes an infringement of any copyright work;

(5) I hereby assign all and every rights in the copyright to this Work to the University of Malaya ("UM"), who henceforth shall be owner of the copyright in this Work and that any reproduction or use in any form or by any means whatsoever is prohibited without the written consent of UM having been first had and obtained;

(6) I am fully aware that if in the course of making this Work I have infringed any copyright whether intentionally or otherwise, I may be subject to legal action or any other action as may be determined by UM.

        Candidate's Signature   Date:

Subscribed and solemnly declared before,

        Witness's Signature   Date:

Name:

Designation:

ABSTRACT

One of the methods of craniofacial anthropometry is indirect anthropometry. A measurement performs on digital facial images or x-ray images. In order to get this measurement, few definable points on structures in individual facial image are needed and mark as landmark points. Currently, most of the work in anthropometric studies uses landmark points that are manually marked on 3D facial image by examiner. This method leads to time consuming and human bias, which will vary within intra-examiner himself and among inter-examiners when involve large data sets. Biased judgment as well leads to a wider gap in measurement error. Thus, this work aims to automate the process of landmarks marking that will help in enhancing the accuracy of measurement.

In this work, automated landmarks detection on 3D human facial image system is produced to identify nasion (*n*), pronasale (*prn*), subnasale (*sn*), alare (*al*), labiale superius (*ls*), stomion (*sto*), labiale inferius (*li*), and chelion (*ch*). These landmarks are detected on 3D human facial image in *.obj* file format and used for obtaining measurements. These measurements are important in craniofacial analysis such that the 3D facial image represents the digital print of the human facial image.

Relationship between 3D geometry characteristic with human feature points is studied. Pronasale (*prn*) are located by searching for vertex with global maximum *z* coordinate while others are located by seeking for local maximum or minimum coordinate at specific region. Fine tuning is implement on certain landmarks by using dot product of two vectors at 3D Euclidean space to improve accuracy.

The system has successfully identify landmarks and obtain measurements with accuracy at nose region is better than orolabial region as landmarks location at orolabial region will be affected by facial expression.

ABSTRAK

Salah satu kaedah antropometri kraniofasial ialah antropometri tak langsung. Pengukuran dilakukan pada imej muka digital atau imej x-ray. Untuk mendapatkan ukuran, beberapa titik ditentukan pada struktur dalam imej muka individu diperlukan dan ditanda sebagai titik tanda. Kebanyakan kerja dalam kajian antropometri menggunakan titik tanda yang ditanda oleh pemeriksa pada imej muka 3D secara manual. Kaedah ini memakan masa dan keberatan sebelah manusia akan wujud dalam pemeriksa sendiri atau antara pemeriksa apabila melibatkan set data yang besar. Pertimbangan berat sebelah akan membesarkan jurang kesilapan pada ukuran. Oleh itu, kerja ini adalah untuk mengautomasikan proses tandaan yang boleh meningkatkan ketepatan ukuran.

Dalam kerja ini, system pengesan tandaan pada imej muka manusia 3D dihasilkan untuk mengenalpasti nasion (n), pronasale (prn), subnasale (sn), alare (al), labiale superius (ls), stomion (sto), labiale inferius (li), dan chelion (ch). Tandaan ini dikesan pada imej muka manusia 3D dalam format fail *.obj* dan digunakan untuk mendapat ukuran. Ukuran ini adalah penting dalam analisis kraniofasial memandangkan imej muka 3D merupakan cetakan digital imej muka manusia.

Hubungan antara ciri-ciri geometri 3D dengan titik ciri manusia dikaji. Pronasale (prn) didapat dengan mencari bucu yang mempunyai koordinat z maksimum global manakala yang lain didapat dengan mencari koordinat maksimum atau minimum tempatan pada rantau tertentu. Penalaan halus dibuat pada tandaan tertentu dengan menggunakan perkalian titik dua vector pada ruang Euklidan 3D untuk meningkatkan ketepatan.

Sistem ini telah berjaya mengenalpasti tandaan dan mendapat ukuran dengan ketepatan pada rantau hidung lebih baik daripada rantau mulut kerana lokasi tandaan pada rantau mulut akan dipengaruhi oleh ekspresi wajah.

ACKNOWLEDGEMENTS

TABLE OF CONTENTS

LIST OF FIGURES

LIST OF TABLES

CHAPTER I

INTRODUCTION

1.1   Background

Craniofacial anthropometry is a science of measuring human face and skull. There are two methods of craniofacial anthropometry, which are direct anthropometry and indirect anthropometry. Farkas, 1981 categorized the act of measurement with the need for physical contact with the subject as direct anthropometry. This manual measurement of physical examination is a tiring process since it is time consuming, dependent on the cooperation of the subject and skill of the clinician. For indirect anthropometry, photograph or 3D image of human face is captured by using camera system. Then measurement is performed on photograph or 3D image.

1.2   Problem Statement

Most of the works in anthropometric studies use landmark points that are manually marked on 3D facial. This method leads to time consuming and bias, which will varies within intra-examiner himself and among inter-examiners when involve large data sets. Biased judgment leads to wider gap in measurement error. Besides that, it is time consuming task. The currently available systems are still said to have many limitations, particularly in domain – specific applications, such as facial image retrieval (Alattab & Kareem, 2012). This work aims to improve upon the previous work limitations in term of recognition accuracy, dimensionality reduction and implementing 3D environment as fully foundation for craniofacial analysis instead of 2D environment.

Majority of previous works fully utilizes 2D, make little or no attempt to maximize sources of 3D facial data in their study sample and employ it in their responding methods.

1.3 Objective

The objective of this project is to develop a system that able to detect human facial landmarks and obtain measurements from 3D facial image automatically. These measurements are important in craniofacial analysis as the 3D facial image represents the digital print of the human facial image.

1.4 Scope

As mentioned in (Othman, Ahmad, Asi, Ismail & Rahman, 2014), there are four regions of the craniofacial complex which are face, orbits, nose and orolabial areas with 18 facial landmarks. However, in this work, automated landmark detection system is produced to detect only eight landmarks namely nasion (*n*), pronasale (*prn*), subnasale (*sn*), alare (*al*), labiale superius (*ls*), stomion (*sto*), labiale inferius (*li*), and chelion (*ch*) which are representing nose and orolabial regions on 3D human facial image in wavefront object (*.obj*) file format.

Once all the above eight landmarks are identified, linear measurement is acquired for height of the nose (*n-sn*), width of the nose (*al-al*), nasal tip protrusion (*sn-prn*), width of the mouth (*ch-ch*), height of the upper lip (*sn-sto*), vermilion height of the upper lip (*ls-sto*), height of the cutaneous upper lip (*sn-ls*), and vermilion height of the lower lip (*sto-li*).

After obtained linear measurements above, proportional indices are calculated for nasal index, nasal tip protrusion width index, upper lip width index, skin portion upper lip index, and upper vermilion height index.

1.5 Significance

The purpose of this research is to design an automated landmarks detection system which able to detect human facial feature points on 3D mesh images and calculate the measurement automatically. The landmarks are identified by using computer algorithm which is free from human bias. Besides that, non-training personnel will able to perform measurement on 3D human facial images accurately within very short time. Thus, more resources and man power will allocate for craniofacial anthropometry studies instead of obtaining the measurement.

1.6 Research Report Organization

This research report is divided into six chapters. Chapter 1 gives the introduction on the background of this research project and the intention of designing automated landmarks detection system. Chapter 2 provides the literature review of this study. Meanwhile chapter 3 describes system requirement and proposed technique to develop automated landmarks detection system. Chapter 4 explains methodology used to accomplish this system development. Results and justification are discussed in chapter 5. And lastly in chapter 6, limitation is described and future enhancement is proposed. A conclusion is given at the end of this chapter.

CHAPTER II

LITERATURE REVIEW

2.1 Introduction

A literature review was conducted on 3D images, craniofacial anthropometry, and automated landmarks techniques. Emphasize is given to the application of automated landmarks detection techniques on the 3D human facial image.

2.2 3D Images

Any object that has height, width and depth is three dimensional object. A 3D mesh image is a collection of vertices, edges and faces (see Figure 2.1) that defines the shape of 3D object. Vertex is defined by x, y, and z coordinates in 3D Euclidean space as shown in Figure 2.2. An edge is a connection between two vertices. A face is a closed set of edges, in which a triangle face has three edges. A polygon triangulation is a subdivision of a given polygon into triangles meeting edge to edge, again with the property that the set of triangle vertices coincides with the set of vertices of the polygon. Resolution of 3D mesh image is depended on the amount of polygon used to construct the object as shown in Figure 2.3.
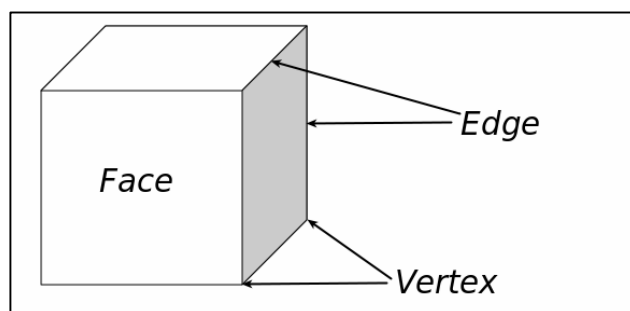
Figure 2.1: Vertex, Edge and Face
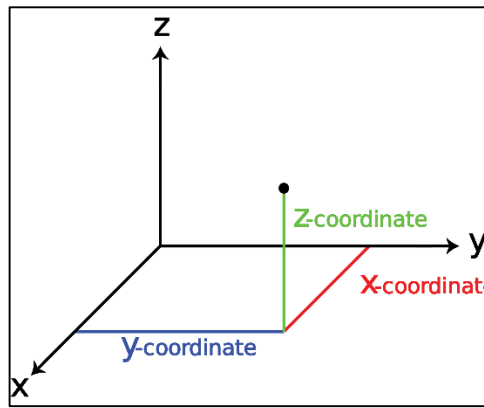
Figure 2.2: Vertex Location in 3D Euclidean Space Using Coordinate System
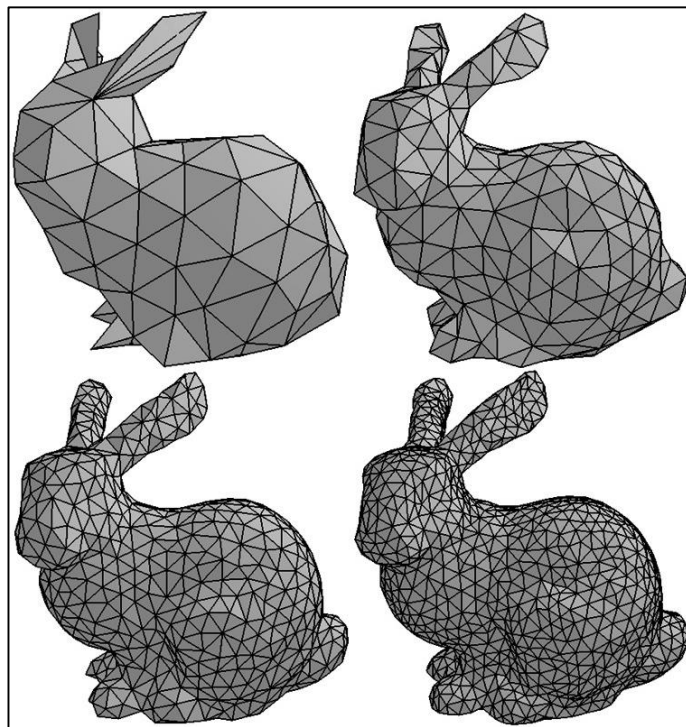
Figure 2.3: 3D Mesh Images of Rabbit with Different Resolution

2.3 Craniofacial Anthropometry

Anthropometry is the science of measuring the human body and its parts. The purpose of anthropometry is to understand human physical variation. Craniofacial anthropometry involves measurement of human face and skull. Craniofacial anthropometry provides a simple and non-invasive method of quantitative assessment of changes in the surface anatomy of the face in individuals.

In a study of relationship between craniofacial parameters and total body height (Anibor, Eboh, & Etetafia, 2011), direct anthropometry approach was used to obtain craniofacial parameters by using non-elastic tape rule, digital vernier calliper and spreading callipers from 200 subjects (100 males and 100 females) that are chosen at random.

Craniofacial anthropometric analysis in Down's syndrome patients (Bagic & Verzak, 2003) has been done. 104 Caucasian individuals with Down syndrome have been investigated. Direct anthropometry is performed by a measurer to obtain 25 craniofacial measurements per patient. 20 to 30 minutes are taken to complete measurement for a cooperative patient.

A study has been done on morphometric characteristics of craniofacial features in patients with schizophrenia (Fakhroddin, Ahmad, & Imran, 2014). In the study, 68 male and 33 female patients with chronic schizophrenia (based on DSM-IV criteria) and 50 male and 51 female healthy volunteers were selected. Craniofacial measurements are obtained directly on patients and volunteers by using Mutitoya 193 digital callipers and Seca S201 anatomical tape measure-ses007. Measurements were done by two people to ensure further accuracy.

In the anthropometric study on patterns of dysmorphology in Crouzon syndrome (Kolar, Munro, & Farkas, 1988) and surface morphology in Treacher Collins syndrome (Kolar, Munro, & Farkas, 1985), anthropometric measurements were obtained from 61 patients and 18 patients correspondingly by using direct anthropometry approach. All measurements were taken by Farkas alone for consistency of results. However, not all measurements were taken due to non-cooperation of some patients.

Facial attractiveness was quantified (Edler, Agarwal, Wertheim, & Greenhill, 2006) by Farkas' proportion indices. In the study, 15 facial photographs of orthognathic

patients were identified. All the photographs were taken by same medical photographer. After that, landmarks were identified on photographs manually.

In a research on 3D head anthropometric analysis (Enciso, Shaw, Neumann, & Mah, 2003), 3D images were acquired by using Eyetronics. Eyetronics is a light-based imaging system consists of a regular slide projector, a digital camera and a calibration pattern. Landmarks are pre-labelled on a mannequin head with small triangle, red colour paper with a blue dot placed on landmarks location. Imaging is performed on the mannequin head and landmarks coordinate are retrieved. Measurements are computed by 3D Euclidian distance between landmarks after anthropometric landmarks are identified and localized.

From the literature review, anthropometry can be divided into two methods which are direct anthropometry and indirect anthropometry. Both methods share some similarities and with some differences. Both methods required well trained personnel to perform measurements. Accuracy of measurements may differ among examiners when large dataset is involved. Both methods are time consuming and tiring process.

However, indirect anthropometry is better than direct anthropometry. Instead of directly perform measurements on patient face for the case of direct anthropometry, facial image is captured using camera system follow by measurement is performed on captured image for the case of indirect anthropometry. Indirect anthropometry is more convenient compare to direct anthropometry. Once facial image has been captured, measurements can be performed by anyone on anytime. While for the directly anthropometry case, appointment has to be made between dentist and patient in order measurement can be done. Re-measurement is not possible without existence of patients.

2.4   Automated Landmarks Detection Methods

Since manually label the landmarks is a labour intensive process, several automated system has been developed to locale feature points on 2D, 2.5D, and 3D images. 2D image able to visualize width and height while 3D image able to visualize width, height and additional depth information. 2.5D image is the image that only one depth value is provided. For 2D images, intensity or colour information is analysed while for 2.5D or 3D images, geometric characteristic information is analysed. Facial feature detection system can be solely depending on geometry characteristic information or further support by statistical models. As 3D images acquisition system become popular and mature, database of 3D human facial images has increased tremendously.

(Beumer, Tao, Bazen, & Veldhuis, 2006) have explore and compare two landmarking methods. The two methods are the Most Likely-Landmark Locator (MLLL), based on maximizing the likelihood ratio and Viola-Jones detection. MLLL treats landmark finding as a two class classification problem. Verify a location in an image is landmark or not. The texture values in a region surrounding a landmark are the features for the classification. For each location in the ROI the likelihood ratio for location to be the landmark is calculated. The one with the highest score is taken to be the landmark. The MLLL method can be enhanced with a shape correction method, BILBO that can improve detection accuracy.

The second method is Viola-Jones detector (Viola & Jones, 2002). This method uses a combination of Haar-like features to represent the texture information in an image. It is using independently trained detectors for each facial landmark. Learning algorithm based on AdaBoost is used to select a small number of critical visual features and yields extremely efficient classifiers.

Active Appearance Models (AAM) (Cootes, Edwards, & Taylor, 2001) is a method which uses a joint statistical model of appearance and shape. Detectors build on

AAM provide a dense set of facial features, allowing to extracting whole contours of facial parts. Face images marked with points defining the main features are required to build a face model. Procrustes analysis is applied to align the sets of points and build a statistical shape model. Training image is warped to obtain a shape free patch. Then matching is done between new images with model image. After that, iterative model refinement is applied to fine tune appearance model parameters and shape transformation parameters to get better accuracy.

Automatic landmark annotation on 3D human facial images has been done by (Guo, Mei, & Tang, 2013). The system start with a set of raw 3D face scans. Then, the nose tip is first localized using a sphere fitting approach. After that, pose normalization is performed to align sample face to a uniform frontal view. Six most salient landmarks were first manually labelled on a set of training samples. Then, Principal Component Analysis (PCA) is performed to localize these 6 landmarks on sample surfaces and 11 additional landmarks were heuristically annotated afterwards. After that, a reference face is chosen and re-meshed using spherical sampling, and TPS-warped to each sample face using the 17 landmarks points. A dense, biological correspondence is built by re-meshing the sample face according to the reference face. The correspondence is further improved by using the average face as the reference and repeating the registration process. The workflow is shown in Figure 2.4.
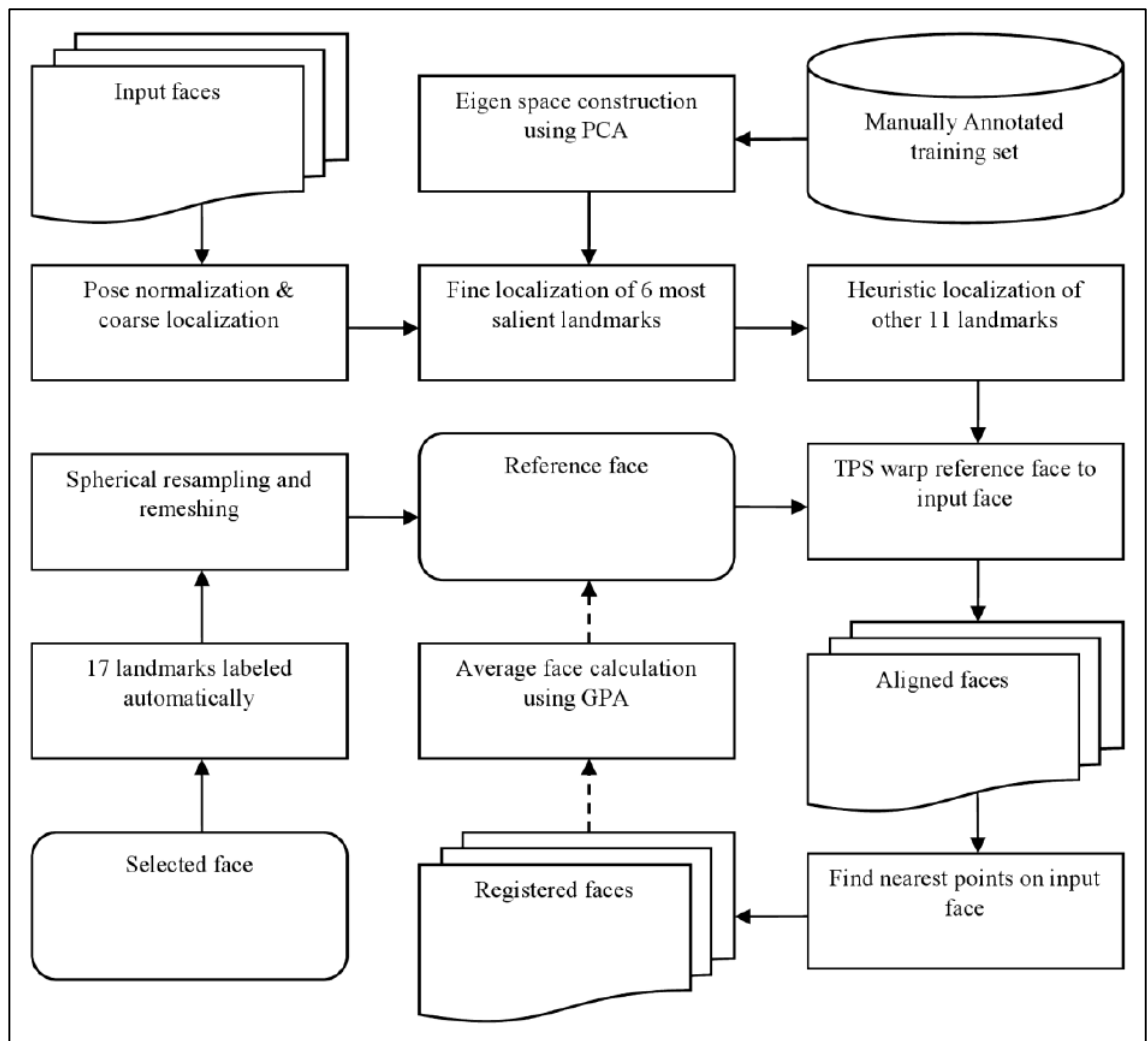
Figure 2.4: The Workflow of the Analysis

(Colombo, Cusano, & Schettini, 2006) method assumes that a 3D shot of a real world scene is available as a range image. Single facial features such as eyes and noses are search initially. Then, a potential face (face triangle) is created from a candidate nose and two candidate eyes. The goal is to discriminate between face triangles that correspond to actual faces and those that do not. The method now registers each candidate face in a standard position and orientation, reducing intra-class face variability. Then, the areas of the range image covered by each face triangle is further analyse by applying a face versus non-face classifier based on a holistic approach. Once the scene is acquired, mean curvature and Gaussian curvature maps are computed from a smoothed version of the original range image. Then, a Mean (H) and Gaussian (K)

classification divides the segmented regions into convex, concave, and two types of saddle regions based on the signs of Gaussian and mean curvature. Regions that may contain a nose and eyes are then characterized by their type and by some statistics of their curvature. This region is rotated and translated into a standard position. Finally, a face versus non-face PCA based classifier is used to process the candidate depth image. The final output of the procedure is a list containing the location and extension of each detected face. Figure 2.5 below shows the steps in this approach.
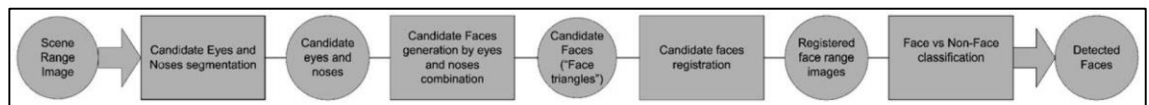
Figure 2.5: Schematic Diagram of Face Detection Method

(Nair & Cavallaro, 2009) use a 3D facial model based on a Point Distribution Model (PDM) to represent the shape of the region of interest that includes the required landmarks, along with statistical information of the shape variation across the training set. A parameterized model is built with PDM to represent each landmark. Training shapes are aligned and scaled to the same coordinate frame to eliminate global transformations. Then, statistical analysis is performed on shape variations by using Procrustes analysis and Principal Component analysis (PCA). After that, statistical information obtained with the PDM is used to test candidate positions on a new mesh to detect faces, landmarks and facial regions. To fit the model, candidate vertices on a face mesh is isolated by using curvature based feature maps. The inner eye and nose tip areas on a face are normally unique based on local curvature and can be robustly isolated from other vertices. The block diagram of the model fitting algorithm is shown in Figure 2.6.
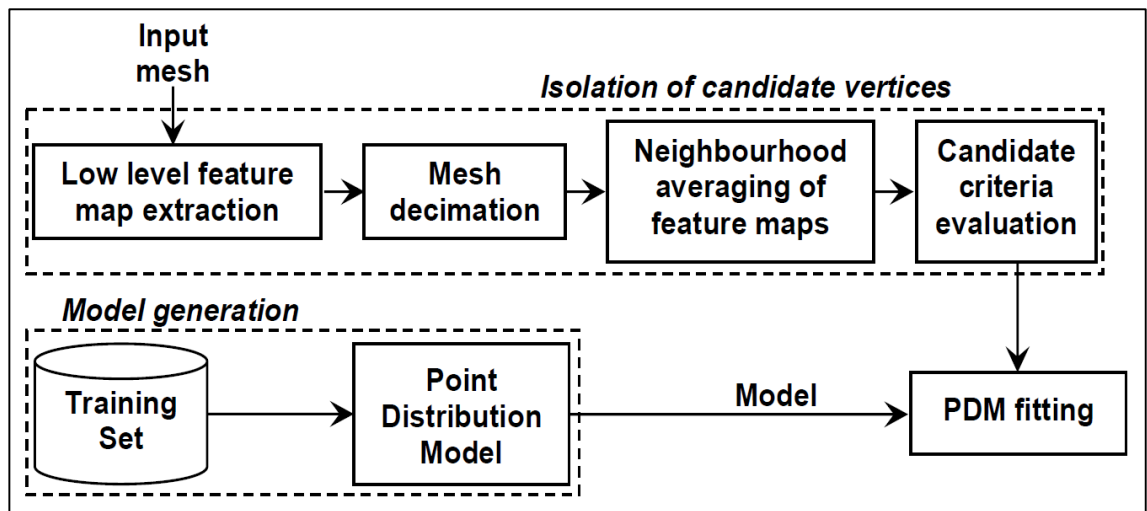
Figure 2.6: Block Diagram of the Model Fitting Approach

Figure 2.7 shows main workflow has been done by (Creusot, Pears, & Austin, 2011). The framework is composed of offline and online processes. The offline part is used to teach the system to look for shape of interest. 14 landmarks over the training set are used to define a dictionary of local shapes from which statistical distributions of descriptors are learnt. The 14 landmarks used are shown in Figure 2.8.

The offline process provides the online system with parameters of the descriptor distributions for a set of landmarks and the weights to linearly combine individual matching score maps. In the online process, D descriptor maps are computed from the input mesh, each value is matched against the 14 learnt descriptor distributions to get score maps with values between 0 and 1. For each landmark, the D descriptor score maps are combined using the learnt weights. The 14 normalised mixed descriptor maps are combined into a single final map, using the maximal value at each vertex. The output keypoints are the local maxima detected on this final map that are above some given threshold.
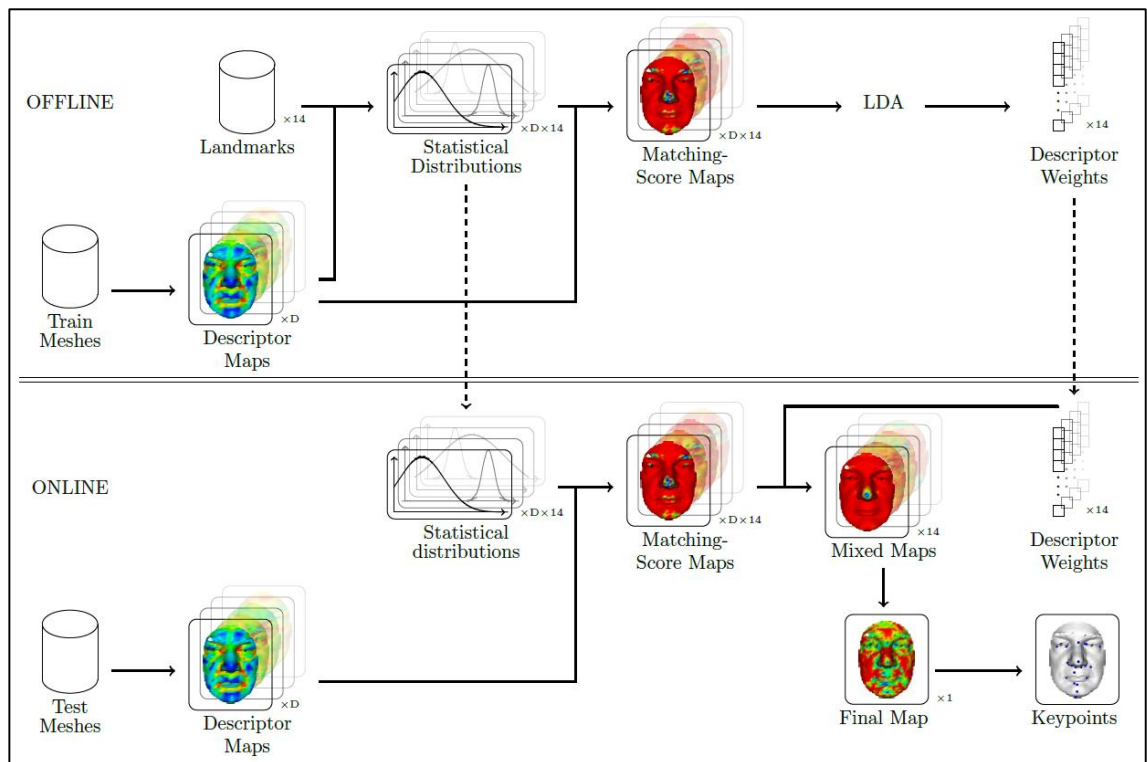
Figure 2.7: Offline Process and Online Process

0 - Left exocanthion (Outer Eye Corner)
1 - Left endocanthion (Inner Eye Corner)
2 - Nasion (Nose Bridge)
3 - Right endocanthion (Inner Eye Corner)
4 - Right exocanthion (Outer Eye Corner)
5 - Pronasale (Nose Tip)
6 - Left Alar Crest Point (Nose Corner)
7 - Right Alar Crest Point (Nose Corner)
8 - Subnasale
9 - Left Cheilion (Mouth Corner)
10 - Right Cheilion (Mouth Corner)
11 - Labiale Superius (Upper lip)
12 - Labiale Inferius (Lower lip)
13 - Pogonion (Chin)
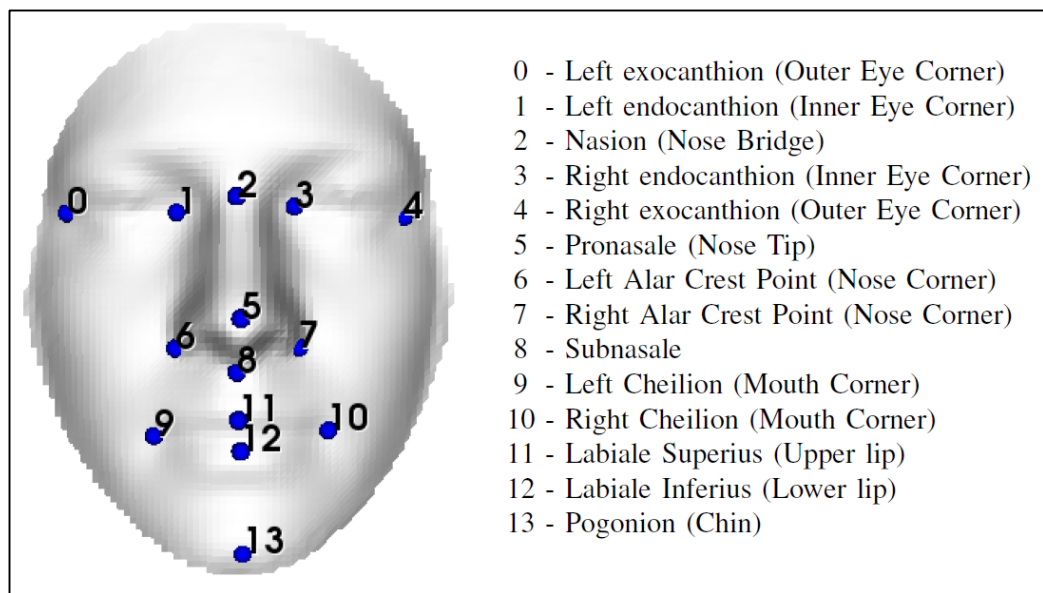
Figure 2.8: Position of Landmarks Used as Shape of Interest

(Lu & Jain, 2006) has made an assumption that nose tip is the closest point to the range camera. They found that nose tip can be easily detected if there is no excessive tilt or yaw of the 3D human facial image.

(Gokberk, Irfanoglu, & Akarun, 2006) has propose an average face model. All landmarks are predefined on average face model. Landmarks registration is done by aligning the 3D human facial image with average face model by using iterative closest point algorithm. After that, fine tuning is done by using shape descriptors such as mean curvature, Gaussian curvature, and etc.

(Boehnen & Russ, 2005) have used both 2D and 3D image information to identify landmarks. Registered 2D colour and range image of face is used. Their algorithm is focus on 2D colour information for better execution speed.

2.5   Summary

This chapter provides the findings of the craniofacial anthropometry and landmarks detection methods in the research area field. A lot of work has been done by various researches to enhance accuracy of identified landmarks.

CHAPTER III

SYSTEM REQUIREMENT AND ANALYSIS

3.1   Users of the System

The system can be used by anyone with minimal computing knowledge. No well-trained examiner is necessary to use this system.

3.2   Functional Requirements

A user friendly system that able to read and visualize 3D image in *OBJ* file format. 3D image can be visualized from any viewpoint by mouse interaction. Zoom and rotation of 3D image can be done using mouse interaction.

Besides that, the system shall able to identify and label craniofacial landmarks automatically. Landmarks identification is done by computer algorithm and consistence for all images without human bias or misjudgement.

In addition, the system will shows coordinate for all landmarks, linear measurements and proportional indices. The results can be saved as *CSV* file format for statistical studies in future.

3.3   Proposed Technique

As stated in chapter 1, the objective of this project is to develop an automated landmarks detection system on 3D human facial image. To achieve this objective, landmarks are identified using 3D geometry shape characteristic information. These facial landmarks are as shown in Figure 3.1 and Figure 3.2. After landmarks are located,

linear measurements are computed using 3D Euclidean distance. Then proportional indices are computed from ratio of linear measurements.
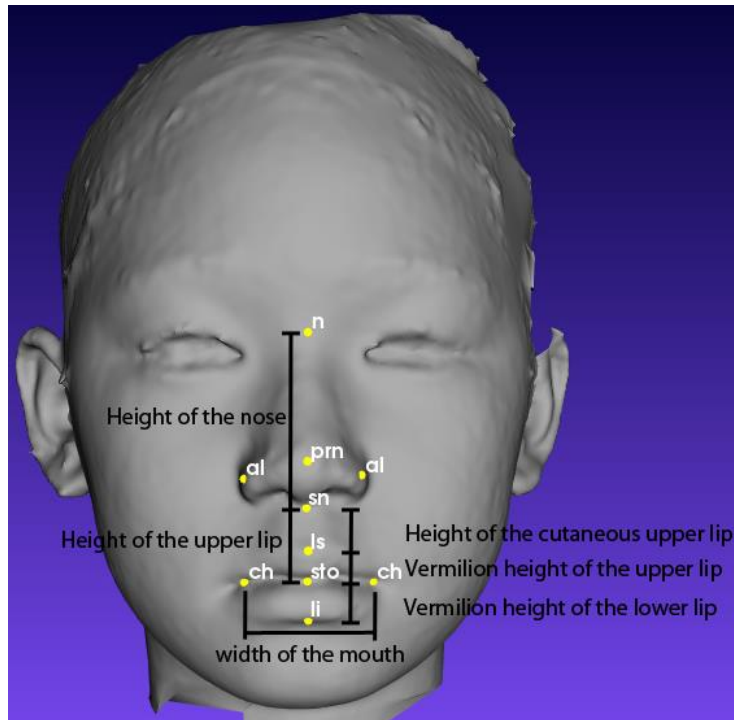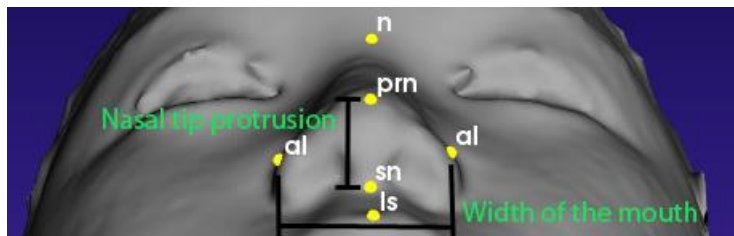

Figure 3.1: Facial Landmarks and Measurements

Figure 3.2: Facial Landmarks and Measurements

CHAPTER IV

MATERIALS AND METHODS

4.1   Materials

There are two types of materials needed in this development. These materials are for image acquisition and system development.

4.1.1   Image Acquisition

A database of raw 3D facial images, acquired from a 3D stereophotogrammetry system during data acquisition is used as data sample. The 3D facial images are obtained by using a stereophotogrammetry camera which is available at the 3D Imaging Lab, Paediatric Dentistry and Orthodontics, Faculty of Dentistry, University of Malaya.

The Vectra M5 CRANIO-3D System as shown in Figure 4.1 is a three dimensional stereophotogrammetry camera system which consist of five cameras. A subject is seated and positioned at the centre of the camera system. They are required to wear a head cap in order to cover their hair. For males, shave is required. This is because the camera unable to retexture any facial hair.

This set of cameras is linked to a desktop computer with specially designated software known as mirror software. Generally, mirror software is used for 3D image capturing, mapping and processing such as to view the facial images, annotating the landmarks manually, measuring the distance and other image simulations.

As shown below in Figure 4.2 is a raw, unprocessed 3D facial images in front view and profile view, without any landmarks are annotated. These 3D facial images will be used for data sample.
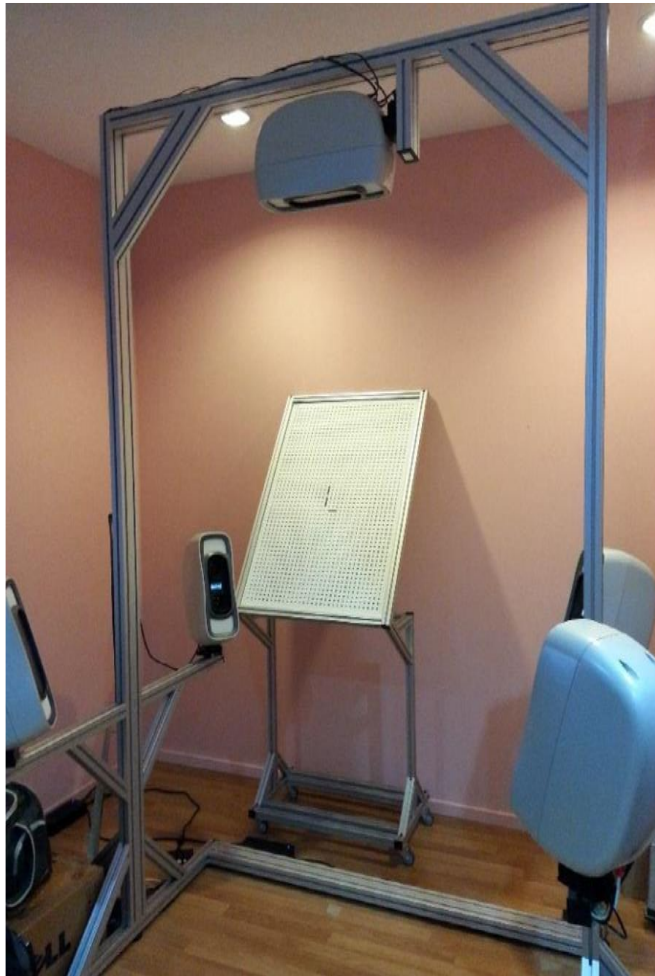

Figure 4.1: Vectra M5 CRANIO-3D System

Figure 4.2: Front and Profile View of 3D Facial Image

4.1.2   System Development Environment

Both hardware and software are necessary for developing automated landmark detection system on 3D human facial image.

A laptop with specification as shown in Table 4.1 is used to design, debug and test the application.

Table 4.1: Development Hardware Specification

Processor	Intel ® Core™ i7-4700MQ CPU @ 2.40 GHz (6MB Cache, up to 3.4 GHz, 4 cores)
Operating System	Windows 8.1 Single Language (64Bit) English
Memory	8GB 800MHz DDR3 SDRAM
Storage	1TB 5400 rpm SATA Hard Drive
Graphic Card	NVIDIA® GeForce® GT 755M 2GB GDDR5

Programming language used in this development is C++. C++ is chosen in this development because C++ was built specifically for platform independence. Furthermore, a lot of open source project and library are contributed and written in C/C++ language. Moreover, application which is developed using C++ language has better execution speed compare to others programming language.

Compiler is used to transforms source code written in C++ language into an executable program. Compiler used in this project is Visual C++ 2013 (known also as Visual C++ 12.0) version number 18.0.21005.1 because target system is running windows operating system.

Qt framework version 5.3.1 is used to design the graphic user interface of the application. Qt is chosen because it is an open source cross platform application framework that can be run on various software and hardware platforms with little or no change in the source code, while having the power and speed of native application.

Visualization Toolkit (VTK) version 6.1.0 is used to visualize the 3D human facial image with landmarks. VTK is an open source cross platform software system for 3D computer graphics visualization. VTK consists of C++ class library and it support a wide variety of visualization algorithms such as scalar, vector, tensor, texture, and volumetric methods. It also support advanced modelling techniques such as implicit modelling, polygon reduction, mesh smoothing, cutting, contouring, and Delaunay triangulation.

CMake version 3.0.2 is used to generate Makefiles and workspaces that locate and include Qt framework library and VTK library as build libraries for Microsoft Visual C++ (MSVC) compiler compilation during building process. CMake is necessary because VTK is open source projects that require cross platform build environment. Besides that, VTK is only available in source code. In the process of building VTK binary, CMake is used to configure and generate build systems such as Makefiles and Visual Studio project files automatically.

Qt Creator version 3.1.2 is an integrated development environment (IDE) used to create source code, build executable application, and debug the application. Qt Creator is chosen because it is part of software development kit (SDK) for Qt framework. Moreover, Qt Creator has built in tools that support CMake wizard.

4.2   Methods

4.2.1   3D Image

A 3D image consists of a set of vertices. Vertices are defined by x, y, and z coordinates in 3D Euclidean space. Figure 4.3 below shows all vertices in a 3D human facial image. Surface is form by forming triangle mesh with three vertices.
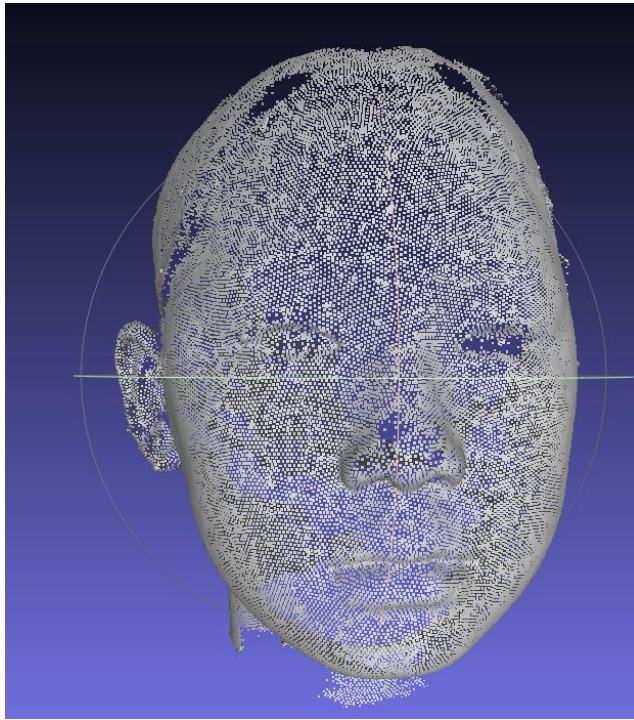
Figure 4.3: Vertices of 3D Image

4.2.2   Automated Landmarks

3D human facial images are representing in Wavefront *OBJ* file format. The Wavefront *OBJ* format represents polygonal data in text form and files are stored with the extension ".obj".

An OBJ file contains several types of definitions. Lines beginning with a hash character (#) are comments. Lines beginning with letter "v" are vertices geometric position in space. The first vertex listed in the file has index 1, and subsequent vertices are numbered sequentially. Lines beginning with letter "vn" are normal. The first normal in the file is index 1, and subsequent normal are numbered sequentially. Lines

beginning with letter "vt" are textures coordinates. The first texture coordinate in the file is index 1, and subsequent textures are numbered sequentially. Lines beginning with letter "f" are polygonal faces. The numbers are indices into the arrays of vertex positions, texture coordinates, and normal respectively.

```
# Comment
v -46.1555 -34.2884 68.0852
v -46.4674 -35.5145 68.3224
              .
              .
vn -0.815296 0.158316 0.556982
vn -0.814482 0.136371 0.563935
              .
              .
vt 0.254987 0.266625
vt 0.251781 0.267134
              .
              .
f 41021/42063/41021 41020/42062/41020 41022/42064/41022
f 41022/42064/41022 41020/42062/41020 41023/42065/41023
              .
              .
```

Figure 4.4: Wavefront *OBJ* File Format

Since *OBJ* file is in text format, regular expression is used to identify lines start with letter "v". Then vertex x, y, z coordinate is extracted and stored in vertices list. After obtaining list of vertices coordinate, maximum z coordinate value is searched. The vertex with maximum z coordinate is pronasale (*prn*).
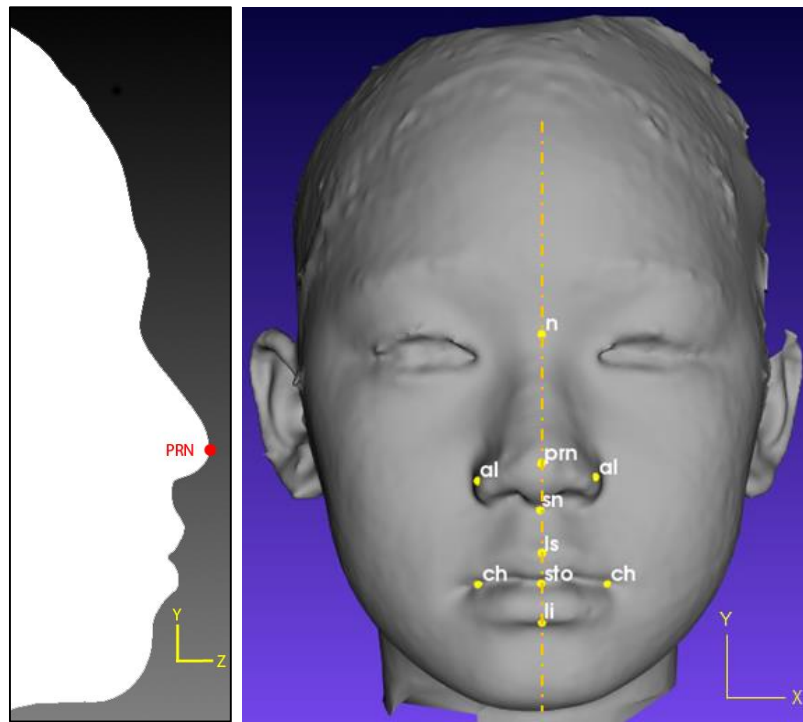
Figure 4.5: Location of Pronasale (*prn*)

After obtaining location of pronasale (*prn*), local z minimum value is searched along the y-axis located at pronasale (*prn*) x coordinate for y value larger than pronasale (*prn*) y coordinate. The vertex with that local z minimum value is nasion (*n*).
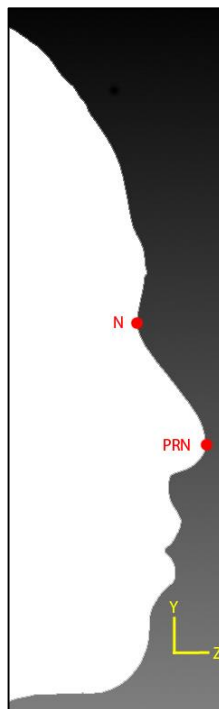

Figure 4.6: Location of Nasion (*n*)

Then, another local z minimum value is searched along the same y-axis located at pronasale (*prn*) x coordinate for y value smaller than pronasale (*prn*) y coordinate. After obtain the vertex with that local z minimum value, angle between three vertices is calculated from that vertex upwards along the same y-axis located at pronasale (*prn*) x coordinate. Vertex with smallest angle is subnasale (*sn*). Formula to calculate angle between three vertices is shown below.

$$3 \; vertices \; A(x,y,z), B(x,y,z), and \; C(x,y,z)$$

$$vector \; \overrightarrow{BA} = \left(A_x - B_x, A_y - B_y, A_z - B_z\right)$$

$$vector \; \overrightarrow{BC} = \left(C_x - B_x, C_y - B_y, C_z - B_z\right)$$

$$Magnitude \; \left\|\overrightarrow{BA}\right\| = \sqrt{(A_x - B_x)^2 + (A_y - B_y)^2 + (A_z - B_z)^2}$$

$$Magnitude \; \left\|\overrightarrow{BC}\right\| = \sqrt{(C_x - B_x)^2 + (C_y - B_y)^2 + (C_z - B_z)^2}$$

$$Normalize \; vector \; \widehat{BA} = \left(\frac{A_x - B_x}{\left\|\overrightarrow{BA}\right\|}, \frac{A_y - B_y}{\left\|\overrightarrow{BA}\right\|}, \frac{A_z - B_z}{\left\|\overrightarrow{BA}\right\|}\right)$$

$$Normalize \; vector \; \widehat{BC} = \left(\frac{C_x - B_x}{\left\|\overrightarrow{BC}\right\|}, \frac{C_y - B_y}{\left\|\overrightarrow{BC}\right\|}, \frac{C_z - B_z}{\left\|\overrightarrow{BC}\right\|}\right)$$

$$\overrightarrow{BA} \cdot \overrightarrow{BC} = \frac{A_x - B_x}{\left\|\overrightarrow{BA}\right\|} \times \frac{C_x - B_x}{\left\|\overrightarrow{BC}\right\|} + \frac{A_y - B_y}{\left\|\overrightarrow{BA}\right\|} \times \frac{C_y - B_y}{\left\|\overrightarrow{BC}\right\|} + \frac{A_z - B_z}{\left\|\overrightarrow{BA}\right\|} \times \frac{C_z - B_z}{\left\|\overrightarrow{BC}\right\|}$$

$$\sphericalangle ABC = \cos^{-1}\left(\overrightarrow{BA} \cdot \overrightarrow{BC}\right)$$
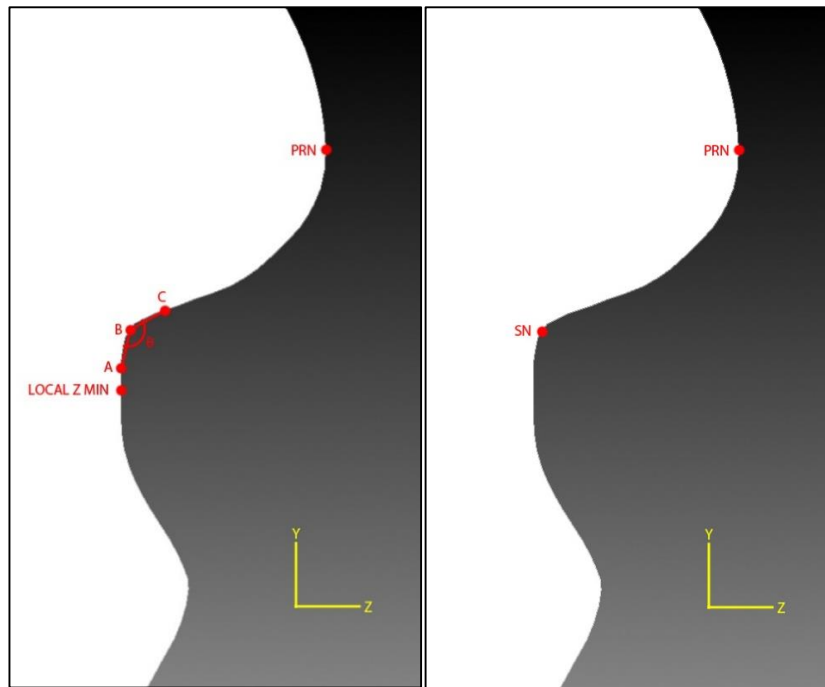
Figure 4.7: Location of Subnasale (*sn*)

After that, from the local *z* minimum, local *z* maximum value is searched downward the same *y*-axis located at pronasale (*prn*) *x* coordinate. The vertex with local *z* maximum value is labiale superius (*ls*). Then from labiale superius (*ls*), local *z* minimum value is searched downward. The vertex with local *z* minimum value is stomion (*sto*).
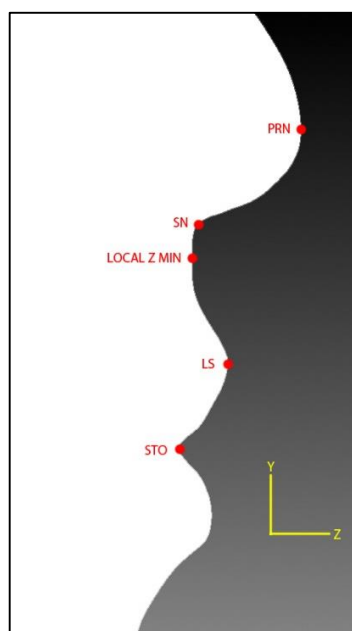
Figure 4.8: Location of Labiale Superius (*ls*) and Stomion (*sto*)

After obtaining stomion (*sto*), another local *z* maximum value is searched downward. After local *z* maximum value is found, by using the same method for obtaining subnasale (*sn*), angle between three vertices is calculated downward. Vertex with smallest angle is labiale inferius (*li*).

Figure 4.9: Location of Labiale Inferius (*li*)

After obtaining pronasale (*prn*) and subnasale (*sn*), vertices which *y* and *z* coordinate value is between subnasale (*sn*) and pronasale (*prn*) *y* and *z* coordinate value are seek. From the seek vertices, vertex with smallest *x* coordinate value is alare (*al*) left while vertex with largest *x* coordinate value is alare (*al*) right.
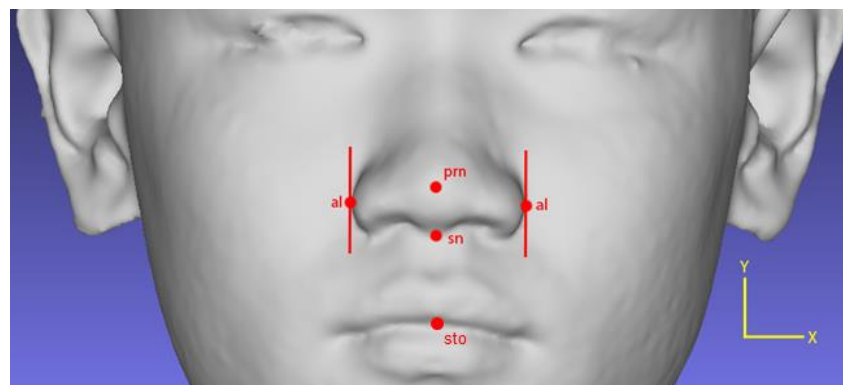

Figure 4.10: Location of Alare (*al*)

After obtaining stomion (*sto*), along the *x*-axis located at stomion (*sto*) *y* coordinate value, angle between three vertices is calculated. Vertex with the smallest angle value to the left of stomion (*sto*) is chelion (*ch*) left while vertex with the smallest angle value to the right of stomion (*sto*) is chelion (*ch*) right.
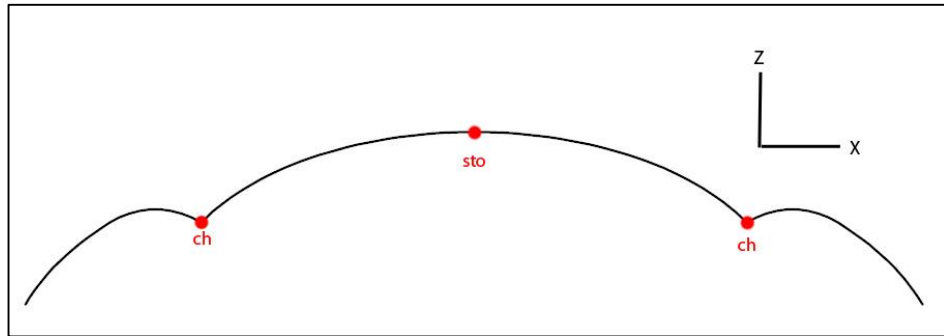
Figure 4.11: Location of Chelion (*ch*)

4.2.3   Measurements

After obtaining landmarks, distance between landmarks is calculated by using Euclidean distance. In three dimensional Euclidean space, if *p = (p1, p2, p3)* and *q = (q1, q2, q3)*, then the distance is given by formula below.

$$d(p,q) = \sqrt{(p_1 - q_1)^2 + (p_2 - q_2)^2 + (p_3 - q_3)^2}$$

Table 4.2 shows the way of getting linear measurements from anthropometric landmarks by using Euclidean distance formula. For example, height of the nose is distance between nasion (*n*) and subnasale (*sn*) while width of the nose is distance between alare (*al*).

Table 4.2: Linear Measurements Derived from Anthropometric Landmarks

Regions	Linear Measurement	Euclidean distance between
Nose	Height of the nose	nasion (*n*) and subnasale (*sn*)
	Width of the nose	alare (*al*)
	Nasal tip protrusion	subnasale (*sn*) and pronasale (*prn*)
Orolabial	Width of the mouth	chelion (*ch*)
	Height of the upper lip	subnasale (*sn*) and stomion (*sto*)
	Vermilion height of the upper lip	labiale superius (*ls*) and stomion (*sto*)
	Height of the cutaneous upper lip	subnasale (*sn*) and labiale superius (*ls*)
	Vermilion height of the lower lip	stomion (*sto*) and labiale inferius (*li*)

After that, proportional indices are calculated according to ratio of linear measurements as shown at the Table 4.3 below.

Table 4.3: Proportional Indices Derived from Linear Measurements

Regions	Proportional Indices
Nose	$Nasal\ index = \dfrac{Width\ of\ the\ nose}{Height\ of\ the\ nose} \times 100$
	$Nasal\ tip\ protrusion\ width\ index = \dfrac{Nasal\ tip\ protrusion}{Width\ of\ the\ nose} \times 100$
Orolabial	$Upper\ lip\ width\ index = \dfrac{Height\ of\ the\ upper\ lip}{Width\ of\ the\ mouth} \times 100$
	$Skin\ portion\ upper\ lip\ index = \dfrac{Height\ of\ the\ cutaneous\ upper\ lip}{Height\ of\ the\ upper\ lip} \times 100$
	$Upper\ vermilion\ height\ index = \dfrac{Vermilion\ height\ of\ the\ upper\ lip}{Vermilion\ height\ of\ the\ lower\ lip} \times 100$

4.3   User Interface Design

The system is built using windows-based. There are two main components which are input and output interface.

4.3.1   Input

The input for the system is 3D facial image. The image is in Wavefront *OBJ* file format.

4.3.2   Output

The system is consisting of two windows. One is for visualizing 3D human facial image with labelled landmarks while another is for showing measurement results. The measurement results can be saved as *CSV* file format. *CSV* file can be opened by any spreadsheet software such as Microsoft Excel.

4.4   Testing Approach

Testing is performed to verify the functionality of the system and accuracy of the detected landmarks.

4.4.1   Functional Test

System testing is performed to verify the functionality of the system. Functional test is executed by using all available 3D images to ensure that the system fulfil functional requirements stated in chapter 3. Functional test is done by preparing a checklist. Step by step procedure is listed down. After that, system testing is done by following the listed procedure as shown in Figure 4.12 and Figure 4.13. Actual results are compared with expected results.

Test case – Detect landmarks on the facial image

Test description:

    To verify the image is uploaded successfully and landmarks is detected

Test execution:

1. Launch application

2. Select Open… from File menu or click Open icon from toolbar (Open File dialog box appears)

3. Choose *OBJ* file and click Open button at the Open File dialog box

Expected results:

1. Coordinate of landmarks location are identified accurately

2. Linear measurement and proportional indices are computed accurately

3. 3D facial image with labelled landmarks able to visualize correctly

Actual results: Pass

1. Location of landmarks able to determine accurately with tolerance

2. Others expected results able to achieve successfully

Figure 4.12: Sample Test Case – Detect Landmarks on Facial Image

Test case – Save the results

Test description:

    To verify the contents of result able to save correctly into *CSV* format

Test execution:

1. Continue from test case above

2. Select Save… from File menu or click Save icon from toolbar (Save File dialog box appears)

3. Choose saving location and type file name. Then click Save button.

Expected results:

    Results able to save correctly into *CVS* format

Actual results: Pass

    Results are saved correctly into *CVS* format

Figure 4.13: Sample Test Case – Save the Results

4.4.2 Accuracy Test

To verify the accuracy of measurements, measurements obtained from system is compared with measurements that obtained manually. Percentage of error is calculated by using formula below.

$$Percentage\ of\ error = \frac{Manual - System}{Manual} \times 100$$

4.4.3 Tester

Since this is not a complex system and 3D images data samples are small, all testing is completed by me.

CHAPTER V

RESULTS AND DISCUSSION

5.1 The System

There are three ways to open a 3D human facial image as shown in Figure 5.1.

- Click 'File' menu then follow by 'Open…'

- Click 'Open' icon on toolbar
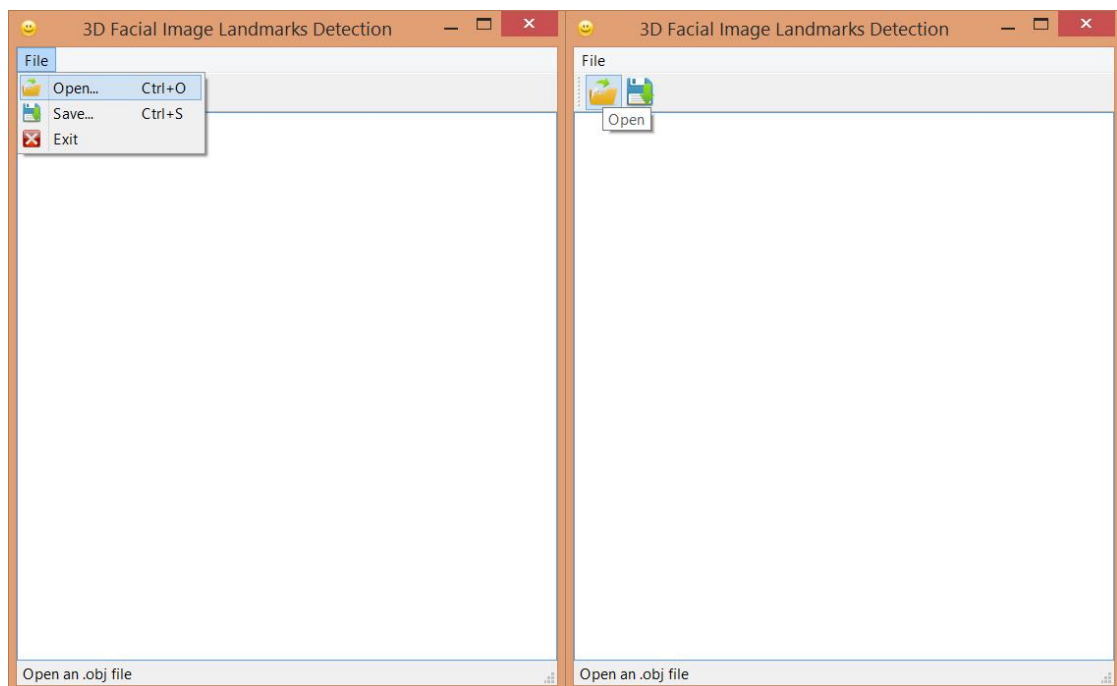
- Press 'Ctrl + O' on keyboard

Figure 5.1: Open 3D Image File

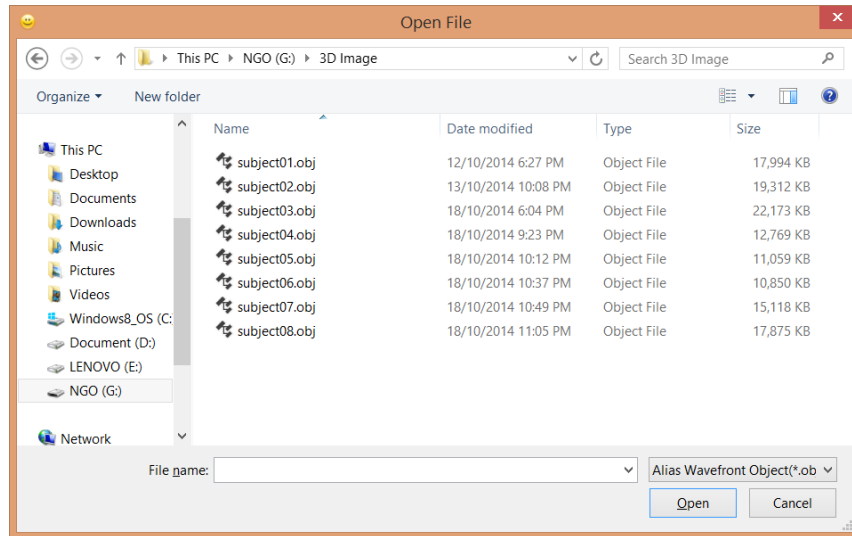After that, following dialogue as shown in Figure 5.2 is appeared.

Figure 5.2: Open File Dialogue

Select an image file in *OBJ* format and click 'Open' button. Two windows are appeared. The left window is used to visualize 3D human facial image with labelled landmarks. Mouse can be used to rotate and zoom in and out the 3D human facial image. The right window is used to show landmarks location, linear measurements, and proportional indices as shown in Figure 5.3.
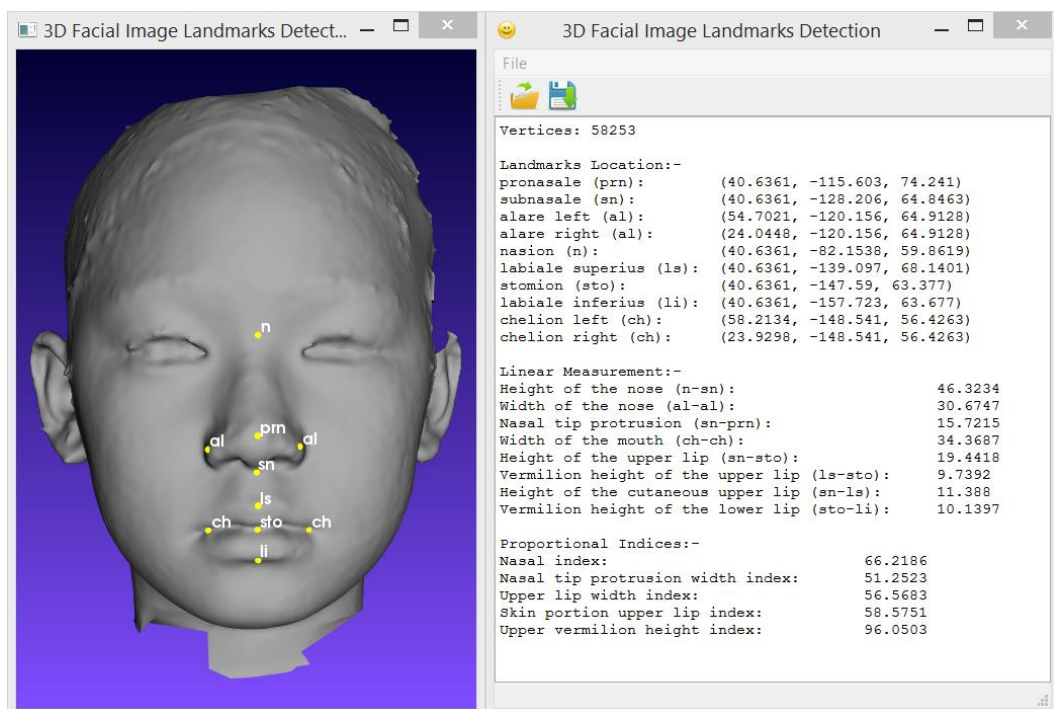

Figure 5.3: Results of the System

Furthermore, results can be saved as 'CSV' file format as well by following ways as shown in Figure 5.4.

- Click 'File' menu then follow by 'Save…'

- Click 'Save' icon on toolbar

- Press 'Ctrl + S' on keyboard
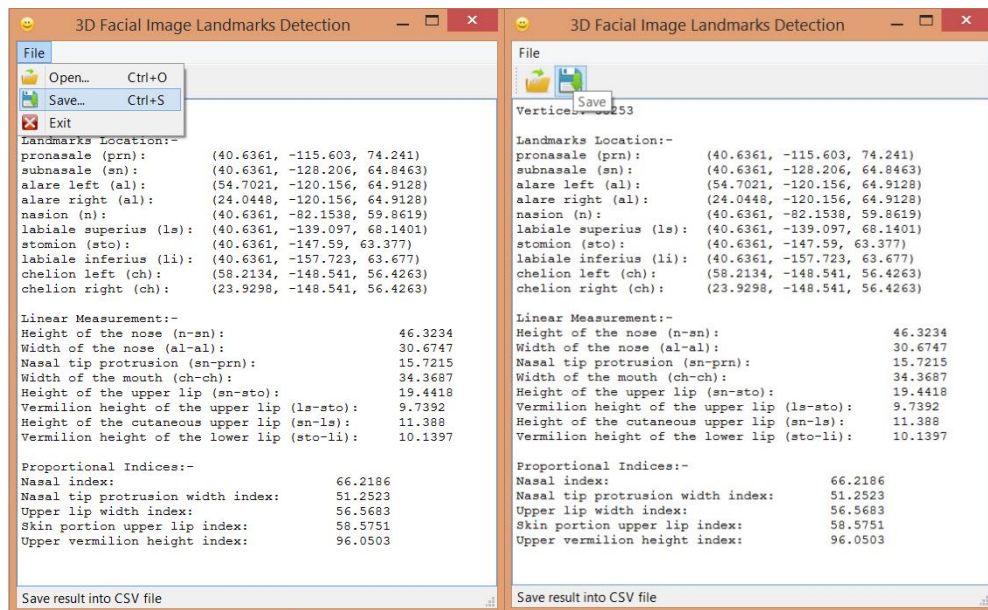
Figure 5.4: Save Results

Following dialogue as shown in Figure 5.5 is appeared. Choose a saved location and type in file name follow by click 'Save' button on the dialogue. Figure 5.6 shows the saved *CSV* file opened with Microsoft Excel.

Figure 5.5: Save File Dialogue

Figure 5.6: Results in *CSV* File Format

5.2 Accuracy Testing Results

Measurements obtain from system are compared with measurements that are obtained manually. The results are shown in Table 5.1.

Table 5.1: Comparison of Measurements between System and Manual

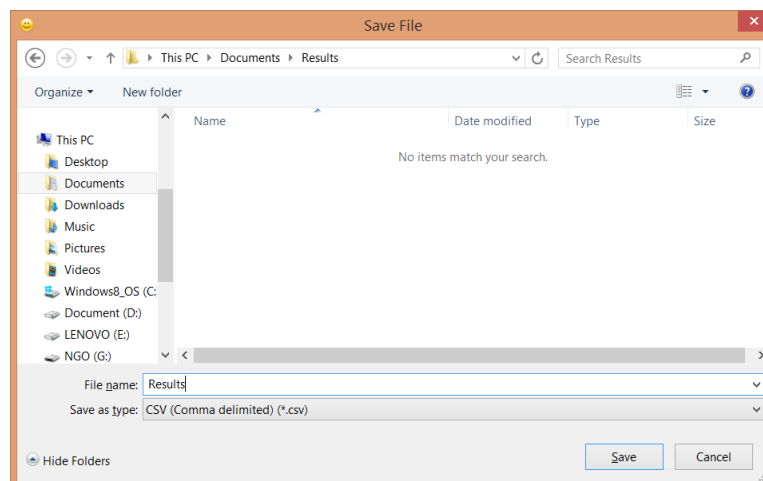| Measurements	Subject 1		Subject 2		Subject 3		Subject 4		Subject 5		Subject 6		Subject 7		Subject 8	
	System	Manual	System	Manual	System	Manual	System	Manual	System	Manual	System	Manual	System	Manual	System	Manual
Height of the nose	47.3536	48	54.8888	54	51.7399	52	36.0344	37	46.3234	47	44.6796	45	45.3647	45	49.1919	50
Width of the nose	34.1817	34	37.7082	37	29.1377	29	34.7777	34	30.6747	30	27.7078	28	30.1876	30	38.3598	38
Nasal tip protrusion	15.7487	15	20.5308	20	14.8126	14	14.1967	14	15.7215	15	12.2913	13	13.9213	14	16.5093	16
Width of the mouth	39.021	42	38.9714	39	35.1013	40	24.4017	30	34.3687	36	28.6649	32	30.4416	35	36.9467	39
Height of the upper lip	21.3718	21	19.1772	19	25.487	25	17.5681	17	19.4418	19	17.3818	17	20.1717	20	21.6332	20
Vermilion height of the upper lip	10.7444	10	9.89845	9	9.26683	9	7.75604	7	9.7392	9	8.29159	8	5.40828	7	11.2629	10
Height of the cutaneous upper lip	13.3044	13	11.6634	12	17.6198	17	13.3351	13	11.388	12	11.7626	11	16.6353	13	13.1503	13
Vermilion height of the lower lip	10.6197	12	9.79888	10	10.8655	11	7.16843	8	10.1397	10	9.22087	9	11.3862	8	7.88133	10

Percentage of error between the system and manual is calculated by using formula below and shown in Table 5.2.

$$Percentage\ of\ error = \frac{Manual - System}{Manual} \times 100$$

Measurements	Percentage of Error							
	Subject 1	Subject 2	Subject 3	Subject 4	Subject 5	Subject 6	Subject 7	Subject 8
Height of the nose	1.3	-1.6	0.5	2.6	1.4	0.7	-0.8	1.6
Width of the nose	-0.5	-1.9	-0.5	-2.3	-2.2	1	-0.6	-0.9
Nasal tip protrusion	-5	-2.7	-5.8	-1.4	-4.8	5.5	0.6	-3.2
Width of the mouth	7.1	0.1	12.2	18.7	4.5	10.4	13	5.3
Height of the upper lip	-1.8	-0.9	-1.9	-3.3	-2.3	-2.2	-0.9	-8.1
Vermilion height of the upper lip	-7.4	-10	-3	-10.8	-8.2	-3.6	22.7	-12.6
Height of the cutaneous upper lip	-2.3	2.8	-3.6	-2.6	5.1	-6.9	-28	-1.2
Vermilion height of the lower lip	11.5	2	1.2	10.4	-1.4	-2.5	-42.3	21.2

Table 5.2: Percentage of Error

5.3 Discussion

The system is able to obtain measurements with error tolerance of ±3% for height of the nose. For width of the nose, measurements error tolerance is ±3% while for nasal tip protrusion, measurements error tolerance is ±6%. Measurements accuracy at nose region are good because nose is a static part on the face, not much movement can be done by nose.

The percentage of error for width of the mouth is varying from 0.1% to 18.7%. The system is facing difficulty to identify correct chelion (*ch*) position for some of the

subject. Surface from left chelion (*ch*) to stomion (*sto*) to right chelion (*ch*) is not a smooth surface. This has cause false positive during identification of chelion (*ch*).

The system able to achieve good accuracy for height of the upper lip with error vary from 0.9% to 3.3% with exception of subject 8 which the error is 8.1%. The system unable to identify stomion (*sto*) location correctly for subject 8 because stomion do not fall on local minimum between labiale superius (*ls*) and labiale inferius (*li*).

Without taking subject 7 and subject 8 into the consideration, percentage error for vermilion height of the upper lip, height of the cutaneous upper lip, and vermilion height of the lower lip vary from 1.2% to 11.5%. Some of the measurement has larger percentage of error because the system unable to locate exact location of stomion (*sto*), labiale superius (*ls*), and labiale inferius (*li*).

For subject 7, the percentage of error for vermilion height of the upper lip, height of the cutaneous upper lip, and vermilion height of the lower lip is very high. Mouth of the subject 7 is opened during image acquisition. The system is unable to get correct measurements if the pose of 3D image is not correct.

CHAPTER VI

FUTURE RECOMMENDATION AND CONCLUSION

6.1   Advantages

The automated landmarks detection system is able to register landmarks on 3D mesh facial images and obtain measurements automatically. In addition, no error causing by human bias will be happened because landmarks registration are performed by same computer algorithm. Consequently, a lot of time has been saved and accuracy has been improved compare to obtain measurement manually. Furthermore, no well trained personnel are necessary to perform this task. Anyone with basic computing knowledge will able to get use of system easily. Therefore, resources such as time and cost for hiring well trained examiner can be saved for craniofacial anthropometry studies instead of obtaining the measurements data.

6.2   Limitation and Future Recommendation

However, the system do has limitation. Input images for the system must be in correct pose and orientation. Therefore, all the 3D facial images must undergo a pre-processing stage before it can be used in the system. In the pre-processing stage, 3D rotation is done manually to the 3D facial images to correct its orientation. An application is made to perform the 3D rotation as shown in Figure 6.1. Following three rotation matrices are used to rotate all vertices in the 3D mesh image for angle θ about *x*, *y* or *z* axis corresponding.

$$R_x(\theta) = \begin{bmatrix} 1 & 0 & 0 \\ 0 & \cos\theta & -\sin\theta \\ 0 & \sin\theta & \cos\theta \end{bmatrix}$$

$$R_y(\theta) = \begin{bmatrix} \cos\theta & 0 & \sin\theta \\ 0 & 1 & 0 \\ -\sin\theta & 0 & \cos\theta \end{bmatrix}$$

$$R_z(\theta) = \begin{bmatrix} \cos\theta & -\sin\theta & 0 \\ \sin\theta & \cos\theta & 0 \\ 0 & 0 & 1 \end{bmatrix}$$
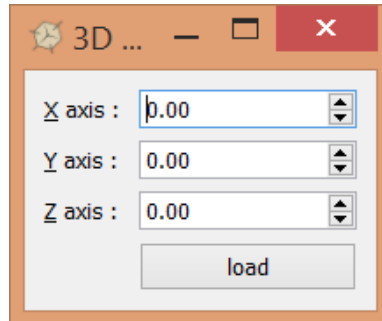

Figure 6.1: 3D Rotation Application for Normalisation

Thus, it cost some time to manually rotate the 3D images. However, time consumption is still less than manually mark feature points on 3D images.

Due to above limitation, future enhancement is necessary. To avoid the necessity of 3D images pre-processing step, the system should be able to find landmarks accurately regardless of orientation. Deformable registration method is recommended for system improvement. In this method, a reference 3D facial mesh model with landmarks is moving around fixed target 3D image to search for best alignment between target and reference image. The moving mesh is allowed to stretch, twist, compress and rotate during the searching process. The reference model and allowable degree of deformed has to be determined by using machine learning method to find out optimum solution for all faces. Deformable registration method is available in image processing software package such as Insight Segmentation and Registration Toolkit (ITK). ITK is an open source, cross platform system that provides developers with an extensive suite of software tools for image analysis.

6.3   Conclusion

In conclusion, the objective for this project has been achieved. The developed system is able to identify landmarks and obtain measurements automatically. Landmarks that able to detect by the system are pronasale (*prn*), nasion (*n*), subnasale (*sn*), labiale superius (*ls*), stomion (*sto*), labiale inferius (*li*), alare (*al*), and chelion (*ch*). The system able to obtain measurements such as height of the nose, width of the nose, nasal tip protrusion, width of the mouth, height of the upper lip, vermilion height of the upper lip, height of the cutaneous upper lip, and vermilion height of the lower lip. The system able to provide proportional indices such as nasal index, nasal tip protrusion width index, upper lip width index, skin portion upper lip index, and upper vermilion height index.

The system is simple and easy to use. Anyone with minimal computing knowledge will able to get used to the system quickly. Therefore, no well-trained examiner is necessary. The landmarks identification process and measurements performed are done automatically within a short moment by using computer algorithm. Consequently, this has help to ease the process of craniofacial anthropometry data collection.

REFERENCES

Alattab, A.A. & Kareem, S.A. (2012). Efficient Method of Visual Feature Extraction for Facial Image Detection and Retrieval. *2012 Fourth International Conference on Computational Intelligence, Modelling and Simulation*, 220-225. doi:10.1109/CIMSim.2012.23

Anibor, E., Eboh, D. E. O., & Etetafia, M. O. (2011). A study of craniofacial parameters and total body height. *Advances in Applied Science Research*, 2(6), 400-405.

Bagic, I. & Verzak, Z. (2003). Craniofacial Anthropometric Analysis in Down's Syndrome Patients. *Collegium Antropologicum*, 27(2), 23-30.

Beumer, G., Tao, Q., Bazen, A. M., & Veldhuis, R. N. J. (2006). A Landmark Paper in Face Recognition. *7th International Conference on Automatic Face and Gesture Recognition (FGR-2006)*. IEEE Computer Society Press.

Boehnen, C. & Russ, T. (2005). A Fast Multi-Modal Approach to Facial Feature Detection. *Application of Computer Vision*, 135-142.

Colombo, A., Cusano, C., & Schettini, R. (2006). 3D Face Detection using Curvature Analysis. *Pattern Recognition*, 39(3), 444-455.

Cootes, T., Edwards, G. J., & Taylor, C. J. (2001). Active Appearance Models. *IEEE Transactions on Pattern Analysis and Machine Intelligence*, 23(6), 681-685.

Creusot, C., Pears, N., & Austin, J. (2011). Automatic Keypoint Detection on 3D Faces Using a Dictionary of Local Shapes. *International Conference on 3D Imaging, Modeling, Processing, Visualization and Transmission (3DIMPVT)*, 204-211. doi:10.1109/3DIMPVT.2011.33

Durtschi, R. B., Chung, D., Gentry, L. R., Chung, M. K., & Vorperian, H. K. (2009). Development craniofacial anthropometry: Assessment of Race effects. *Clinical Anatomy*, 22(7), 800-808. doi:10.1002/ca.20852

Edler, R., Agarwal, P., Wertheim, D., & Greenhill, D. (2006). The use of anthropometric proportion indices in the measurement of facial attractiveness. *European Journal of Orthodontics*, 274-281.

Enciso, R., Shaw, A., Neumann, U., & Mah, J. (2003). 3D head anthropometric analysis. *SPIE Medical Imaging*. Retrieved from http://graphics.usc.edu/cgit/publications/papers/SPIE_jan28.pdf

Fakhroddin, M., Ahmad, G., & Imran, S. (2014). Morphometric characteristics of craniofacial features in patients with schizophrenia. *J Psychiatry*, 17, 514-519.

Gokberk, B., Irfanoglu, M. O., & Akarun, L. (2006). 3D shape-based face representation and feature extraction for face recognition. *Image and Vision Computing*, 24(8), 857-869. doi:10.1016/j.imavis.2006.02.009

Guo, J., Mei, X., & Tang, K. (2013). Automatic landmark annotation and dense correspondence registration for 3D human facial images. *BMC Bioinformatics*, 14(1), 232. doi:10.1186/1471-2105-14-232

Kolar, J. C., Munro, I. R., & Farkas, L. G. (1985). Surface Morphology in Treacher Collins Syndrome: An Anthropometric Study. *The Cleft Palate Journal*, 22(4), 266-274.

Kolar, J. C., Munro, I. R., & Farkas, L. G. (1988). Patterns of Dysmorphology in Crouzon Syndrome: An Anthropometric Study. *Cleft Palate Journal*, 25(3), 235-244.

Lu, X., Colbry, D., & Jain, A. K. (2004). Three Dimensional Model Based Face Recognition. *International Conference on Pattern Recognition*.

Lu, X., & Jain, A. K. (2006). Automatic feature extraction for multiview 3D face recognition. *International Conference on Automatic Face and Gesture Recognition*, 585-590. doi:10.1109/FGR.2006.23

Mian, A.S., Bennamoun, M. & Owens, R. (2007). An efficient multimodal 2D-3D hybrid approach to automatic face recognition. *IEEE transactions on pattern analysis and machine intelligence*, 29(11), 1927-1943. doi:10.1109/TPAMI.2007.1105

Nair, P. & Cavallaro, A. (2009). 3D Face Detection, Landmark Localization, and Registration using a Point Distribution Model. *IEEE Transactions on Multimedia*, 11(4), 611-623. doi:10.1109/TMM.2009.2017629

Othman, S. A., Ahmad, R., Asi, S. M., Ismail, N. H., & Rahman, Z. A. A. (2014). Three-dimensional quantitative evaluation of facial morphology in adults with unilateral cleft lip and palate, and patients without clefts. *British Journal of Oral & Maxillofacial Surgery*, 52(3), 208-213. doi: 10.1016/j.bjoms.2013.11.008

Pears, N., Liu, Y., & Bunting, P. (2012). *3D Imaging, Analysis and Application*. Aberystwyth, UK: Springer.

Uricar, M., Franc, V., & Hlavac, V. (2012). Detector of Facial Landmarks Learned by the Structured Output SVM. *International Conference on Computer Vision Theory and Applications*, 547-556.

Vezzetti, E. & Marcolin, F. (2012). 3D human face description: landmarks measures and geometrical features. *Image and Vision Computing*, 30(10), 698–712. doi:10.1016/j.imavis.2012.02.007

Viola, P. & Jones, M. J. (2002). Robust real-time object detection. *International Journal of Computer Vision*.